Uluslararası İleri Doğa Bilimleri ve Mühendislik Araştırmaları Dergisi
Sayı 8, S. 399-410, 2, 2024

Araştırma Makalesi

IJANSER
https://as-proceeding.com/index.php/ijanser
ISSN: 2980-0811

International Journal of Advanced Natural Sciences and Engineering Researches
Volume 8, pp. 399-410, 2, 2024

Research Article

Pseudo-Static calculation formula for dynamic thrust behind Cantilever retaining wall: Investigating failure plans in C-Φ soil

GHARBI Ayman[*1], EL KHANNOUSSI Fadoua[2], EL YAMOUNI Bouraida[3], KHAMLICHI Abdellatif [4]

[1] *Research team AMSCG, Laboratory ICST, National School of Applied Sciences at Tetouan, Abdelmalek Essaadi University, Morocco, ayman.gharbi@etu.uae.ac.ma*
[2] *Research team AMSCG, Laboratory ICST, National School of Applied Sciences at Tetouan, Abdelmalek Essaadi University, Morocco, felkhannoussi@uae.ac*
[3] *Research team 3M, Laboratory ICST, National School of Applied Sciences at Tetouan, Abdelmalek Essaadi University, Morocco, belyamouni@uae.ac.ma*
[4] *Research team 3M, Laboratory ICST, National School of Applied Sciences at Tetouan, Abdelmalek Essaadi University Department of Industrial and Civil Sciences and Technologies, Morocco, akhamlichi@uae.ac.ma*

(Received: 10 March 2024, Accepted: 12 March 2024)

(4th International Conference on Innovative Academic Studies ICIAS 2024, March 12-13, 2024)

ATIF/REFERENCE: Gharbi, A., El Khannoussi, F., El Yamouni, B. & Khamlichi, A. (2024). Pseudo-Static calculation formula for dynamic thrust behind Cantilever retaining wall: Investigating failure plans in C-Φ soil. *International Journal of Advanced Natural Sciences and Engineering Researches, 8(2), 399-410.*

Abstract – In the design of retaining walls subjected to seismic loads, the pseudo-static method based mainly on the Coulomb approach (equilibrium of forces) is widely used. However, this method does not consider all the complex phenomena observed during the experimental tests, such as tension cracks, the non-linearity of soil response, and the shape of failure surfaces. Therefore, researchers have long been working to develop formulations that take these phenomena into account. This note presents a formulation of the active dynamic thrust applied to a cantilever retaining wall supporting C-Φ soil, considering the shape of the sliding surfaces in the active state. The equation of this formula is based on the pseudo-static approach and considers the vertical and horizontal components of the seismic coefficient.

Keywords – Pseudo-Static Approach, Cantilever Retaining Wall, Failure Surface, Small And Short Heel, Active Dynamic Thrust.

I. INTRODUCTION

Retaining walls are structures designed to support and stabilize the earth, enabling the creation of space for other civil engineering structures such as bridges or roads. When subjected to seismic forces, the response of retaining walls is complex, because several parameters are involved, such as the inclination of soil slopes, the angle of internal friction, cohesion, the shape of failure surfaces, and the hydric state of the soil.

The method for calculating the dynamic force exerted on a retaining wall was initially introduced by Okabé and Mononobé [11-12], based on the Coulomb approach [2], which considers the equilibrium of forces. Although this method has some limitations [15], it is widely used for the dimensioning of retaining structures [5].

Subsequently, the MO method was extended to include the effect of soil cohesion. Several studies have contributed to this extension, such as those by Mazindrani and Ganjali [10], Cheng, 2003 [3]; Puri et al., 2004 [13]; Anderson et al., 2008 [1]; Shukla et al., 2009 [18], Shrestha et al., 2016 [11], Gupta et al., 2016 [16]; Shi et al., 2016 [19]. Most of these methods assume that the shape of the sliding surface is flat and inclined at an angle to maximize the active force.

However, for cantilever walls, the shape of the sliding surfaces varies according to the length of the heels: in the case of a "long" heel, the sliding line intercepts the footing, whereas in the case of a "short" heel, this line reaches the ground surface [9].

Kamiloğlu & Şadoğlu [9] propose formulas for calculating the active dynamic force in both cases: short heel and long heel. This note extends the Kamiloğlu & Şadoğlu [9] study by introducing the effect of cohesion.

II. MATERIAL AND METHOD

The equation of the analytical formulas for the forces acting on the ground wedge varies according to the length of the heel. In the case of a long heel, the failure line reaches the ground surface, whereas in the case of a short heel, this line intercepts the toe. Figure 1 illustrates both cases, also showing the mobilized soil wedge and the forces acting on it.

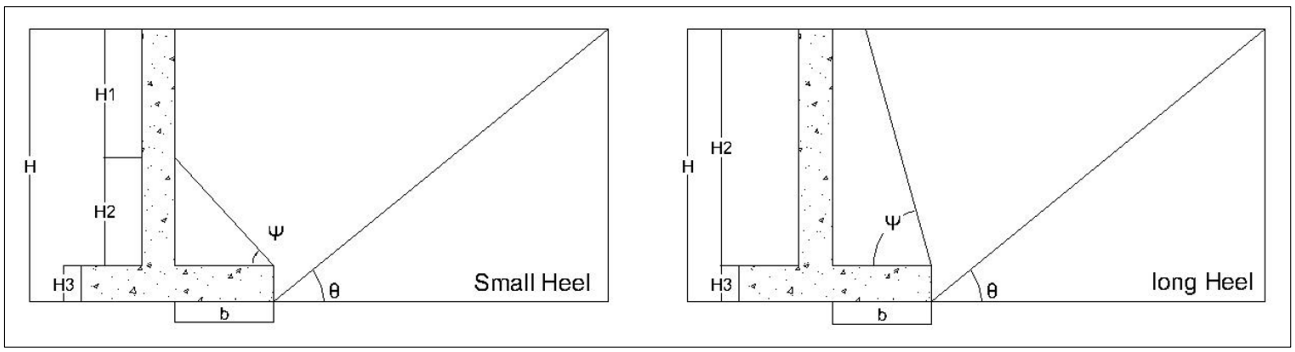

Figure 1. Failure surfaces behind a cantilever retaining wall according to heel length: short heel and long heel [9]

The derivation of the analytical formula is based on the following assumptions: the soil is in a limit state; failure lines are plane; the effect of tension cracking is not considered.

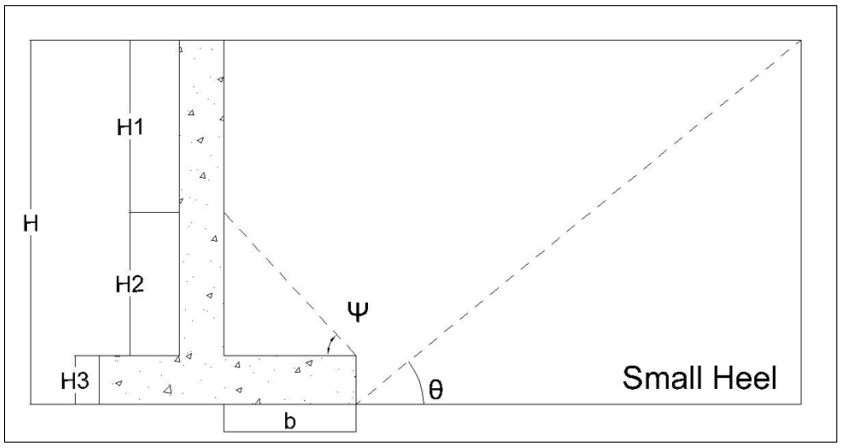

Figure 2. Failure surfaces behind a cantilever retaining wall with a small heel

The various study parameters are as follows: cohesion c, soil internal friction angle Φ, horizontal and vertical seismic coefficients Kv=av/g and Kh=ah/g, the friction angle between soil and wall δ, the inclination angles of the failure planes θ and ψ, α = H3/H, a parameter characterizing the thickness of the heel, β = b/H, a parameter characterizing heel length.

The suffix SH is associated with the parameters in the case of a short heel, and the suffix LH is associated with the parameters in the case of a long heel.

In the case of a wall with a short heel, three forces are applied to the wedge of the soil named ABCDE in Figure 2. It is assumed that the forces Pa1SH and PaSH are inclined by the angle δ, while Pa2SH and R (the soil reaction) are inclined by Φ.

Kamiloğlu & Şadoğlu state in [8-9] that the failure surface noticed in the static state is represented by the line BF, shown in Figure 3.

To determine the first force, Pa1SH, the equilibrium of the ABF soil wedge can be expressed as follows: ΣF = 0, where ΣF represents the sum of the forces acting on the ABF.

Projecting the equilibrium equation on the x-axis and y-axis gives:

$$P_{a1SH}\cos(\delta) + C * BF\cos(\theta) - k_h W_{wedge} - R\cos\left(\frac{\pi}{2} - \theta + \phi\right) = 0 \qquad (1)$$

$$P_{a1SH}\sin(\delta) + C * BF\sin(\theta) - (1 - k_v)W_{wedge} + R\sin\left(\frac{\pi}{2} - \theta + \phi\right) = 0 \qquad (2)$$

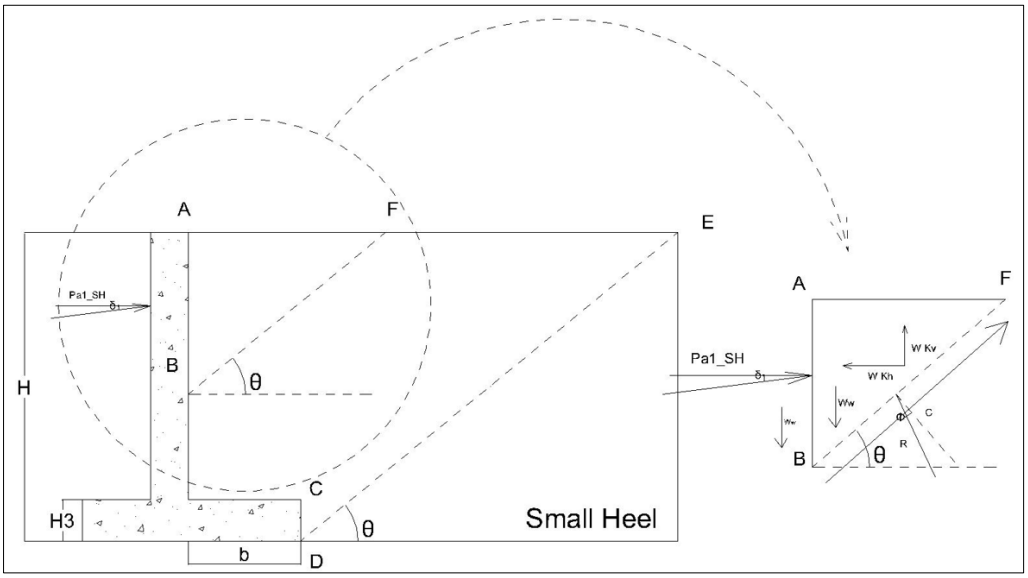

Figure 3. The force Pa1SH acting on the wedge of the soil ABF in the case of a wall with a short heel

Projecting the equilibrium equation on the x-axis and y-axis gives:

$$P_{a1SH}\cos(\delta) + C * BF\cos(\theta) - k_h W_{wedge} - R\cos\left(\frac{\pi}{2} - \theta + \phi\right) = 0 \qquad (3)$$

$$P_{a1SH}\sin(\delta) + C * BF\sin(\theta) - (1 - k_v)W_{wedge} + R\sin\left(\frac{\pi}{2} - \theta + \phi\right) = 0 \qquad (4)$$

Multiplying the first equation (3) by $\sin\left(\frac{\pi}{2} - \theta + \phi\right)$ and the second equation (4) by $\cos\left(\frac{\pi}{2} - \theta + \phi\right)$ and summing them gives :

$$P_{a1SH} = \frac{1}{2} * \gamma H^2 * \frac{(1 - \beta\mathrm{Tan}(\psi) - \alpha)^2 * \cot(\theta)}{\sin\left(\frac{\pi}{2} - \theta + \phi + \delta\right)} * [k_h * \sin\left(\frac{\pi}{2} - \theta + \phi\right) + (1 - k_v)\cos\left(\frac{\pi}{2} - \theta + \phi\right)] - CH * \frac{(1 - \beta\mathrm{Tan}(\psi) - \alpha)}{\sin\left(\frac{\pi}{2} - \theta + \phi + \delta\right)} * \cos(\phi) \qquad (5)$$

The second force to be determined is Pa3SH, to do so, we consider the equilibrium of the CDF soil wedge, which is subjected to the forces shown in Figure 4.

Projecting the equilibrium equation on the x-axis and y-axis gives:

$$P_{a3SH}\cos(\delta) + C * DF * \cos(\theta) - k_h W_{wedge} - k_h W_{surcharge} - R\cos\left(\frac{\pi}{2} - \theta + \phi\right) = 0 \qquad (6)$$

$$P_{a3SH}\sin(\delta) + C * DF * \sin(\theta) - (1 - k_v)W_{wedge} - (1 - k_v)W_{surcharge} - R\sin\left(\frac{\pi}{2} - \theta + \phi\right) = 0 \qquad (7)$$

Multiplying the first equation (6) by $\sin\left(\frac{\pi}{2} - \theta + \phi\right)$ and the second equation (7) by $\cos\left(\frac{\pi}{2} - \theta + \phi\right)$ and summing them gives :

$$P_{a3SH} = \frac{1}{2} * \gamma H^2 * \frac{[2 * \alpha * \cot(\theta) * (1 - 0.5\alpha) * (k_h \sin\left(\frac{\pi}{2} - \theta + \phi\right) + (1 - k_v)\cos\left(\frac{\pi}{2} - \theta + \phi\right))}{\sin\left(\frac{\pi}{2} - \theta + \phi + \delta\right)} - CH * \frac{[\alpha\cot(\theta)\sin\left(\frac{\pi}{2} - \theta + \phi\right) + \alpha\cos\left(\frac{\pi}{2} - \theta + \phi\right)]}{\sin\left(\frac{\pi}{2} - \theta + \phi + \delta\right)} = \frac{1}{2}\gamma H^2 * K_{a\gamma 3SH} - CHK_{ac3SH} \qquad (8)$$

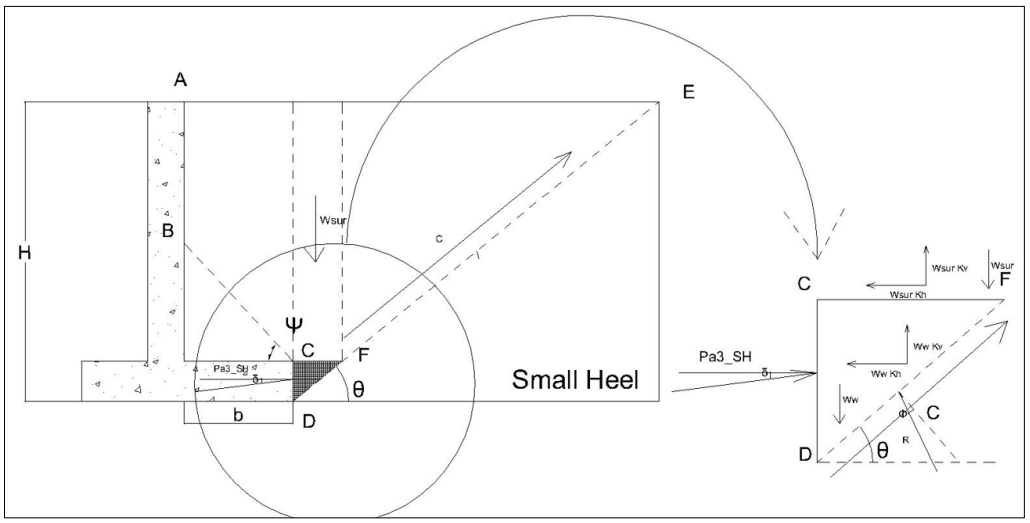

Figure 4. The force Pa3SH acting on the wedge of the soil CDF in the case of a wall with a short heel

The last force to be determined in the case of a cantilever wall with a short heel is Pa2SH. In this case, we consider the global model shown in Figure 5.

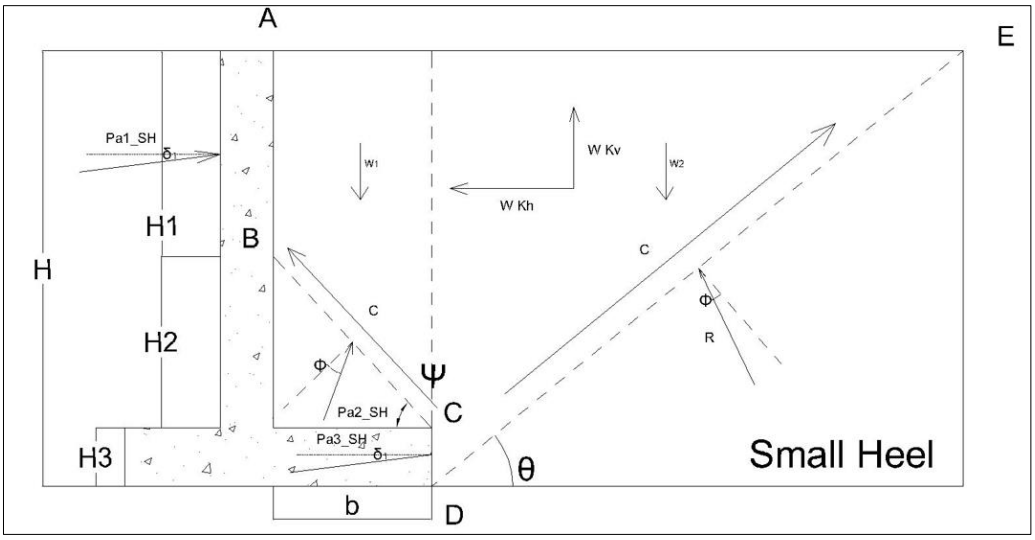

Figure 5. The soil model used to determine the Pa2SH in the case of a wall with a short heel

Projecting the equilibrium equation on the x-axis and y-axis gives:

$$(P_{a3SH} + P_{a1SH})\cos(\delta) + P_{a2SH} * \cos\left(\frac{\pi}{2} - \psi + \phi\right) - C * BC * \cos(\psi) + C * DE * \cos(\theta) - k_h W_1 - k_h W_2 - R\cos\left(\frac{\pi}{2} - \theta + \phi\right) = 0 \quad (9)$$

$$(P_{a3SH} + P_{a1SH})\sin(\delta) + P_{a2SH} * \sin\left(\frac{\pi}{2} - \psi + \phi\right) - C * BC * \sin(\psi) + C * DE * \sin(\theta) - (1 - k_v)W_1 - (1 - k_v)W_2 - R\sin\left(\frac{\pi}{2} - \theta + \phi\right) = 0 \quad (10)$$

Multiplying the first equation (9) by $\sin\left(\frac{\pi}{2} - \theta + \phi\right)$ and the second equation (10) by $\cos\left(\frac{\pi}{2} - \theta + \phi\right)$ and summing them gives :

$$P_{a2SH} = \frac{1}{2} * \gamma H^2 * \{-\frac{\sin\left(\frac{\pi}{2} - \theta + \phi + \delta\right)}{\sin(\pi - \theta + 2\phi - \psi)} * (K_{a\gamma 3SH} + K_{a\gamma 1SH}) + \frac{2[(1 - \alpha - 0.5\beta * \tan(\psi))\beta + 0.5\cot(\theta)]}{\sin(\pi - \theta + 2\phi - \psi)}\theta[k_h \sin\left(\frac{\pi}{2} - \theta + \phi\right) + (1 - k_v)\cos\left(\frac{\pi}{2} - \theta + \phi\right)]\} - CH * \frac{1}{\sin(\pi - \theta + 2\phi - \psi)}\{[(\cot(\theta) * \sin\left(\frac{\pi}{2} - \theta + \phi\right) + \cos\left(\frac{\pi}{2} - \theta + \phi\right)) + \beta(\tan(\psi) * \cos\left(\frac{\pi}{2} - \theta + \phi\right) - \sin\left(\frac{\pi}{2} - \theta + \phi\right))] - (K_{ac3SH} + K_{ac1SH}) * \sin\left(\frac{\pi}{2} - \theta + \phi + \delta\right)\} = \frac{1}{2}\gamma H^2 * K_{a\gamma 2SH} - CHK_{ac2SH} \quad (11)$$

In the case of a wall with a long heel, two forces are applied to the wedge of the soil named ABCDE in Figure 6. It is assumed that the force Pa3SH is inclined by the angle δ, while Pa2SH and R (the soil reaction) are inclined by Φ.

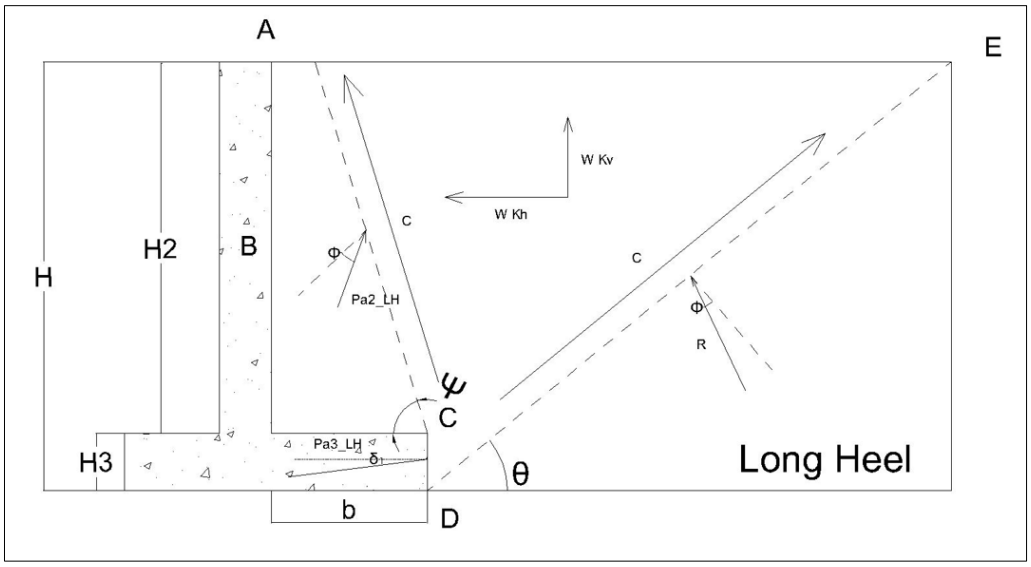

Figure 6. Failure surfaces behind a cantilever retaining wall with long heel

To determine the Pa2LH and Pa3LH forces, we follow the same steps as for a short heel. For Pa3LH, we consider the soil wedge BCD shown in Figure 7.

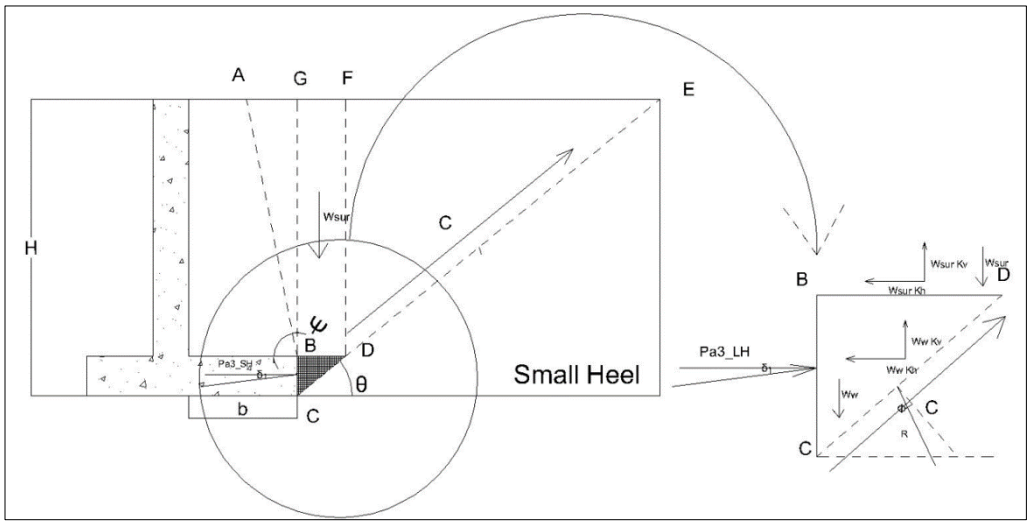

Figure 7. The force Pa3_SH acting on the wedge of the soil BCD in the case of a wall with a long heel

Projecting the equilibrium equation on the x-axis and y-axis gives:

$$P_{a3LH}\cos(\delta) + C * CD * \cos(\theta) - k_h W_{wedge} - k_h W_{surcharge} - R_3 \cos\left(\frac{\pi}{2} - \theta + \phi\right) = 0 \quad (12)$$

$$P_{a3LH}\sin(\delta) + C * CD * \sin(\theta) - (1 - k_v) W_{wedge} - (1 - k_v) W_{surcharge} - R \sin\left(\frac{\pi}{2} - \theta + \phi\right) = 0 \quad (13)$$

Multiplying the first equation (12) by $\sin\left(\frac{\pi}{2} - \theta + \phi\right)$ and the second equation (13) by $\cos\left(\frac{\pi}{2} - \theta + \phi\right)$ and summing them gives :

$$P_{a3LH} = \frac{1}{2} * \gamma H^2 * \frac{[2 * \alpha * \cot(\theta) * (1 - 0.5\alpha) * (k_h \sin\left(\frac{\pi}{2} - \theta + \phi\right) + (1 - k_v) \cos\left(\frac{\pi}{2} - \theta + \phi\right))]}{\sin\left(\frac{\pi}{2} - \theta + \phi + \delta\right)}$$
$$- CH * \frac{[\alpha \cot(\theta) \sin\left(\frac{\pi}{2} - \theta + \phi\right) + \alpha \cos\left(\frac{\pi}{2} - \theta + \phi\right)]}{\sin\left(\frac{\pi}{2} - \theta + \phi + \delta\right)}$$
$$= \frac{1}{2}\gamma H^2 * K_{a\gamma 3LH} - CHK_{ac3LH} \qquad (14)$$

The next force to be determined in the case of a cantilever wall with a long heel is Pa2LH. In this case, we consider the global model shown in Figure 8.

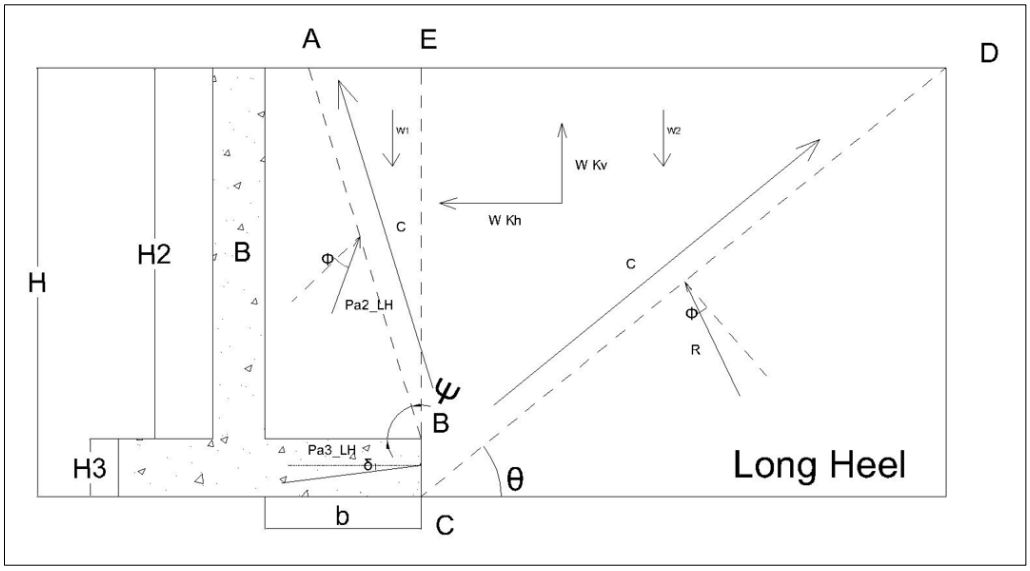

Figure 8. The soil model used to determine the Pa2_SH in the case of a wall with a long heel

Projecting the equilibrium equation on the x-axis and y-axis gives:

$$(P_{a3LH})\cos(\delta) + P_{a2LH} * \cos\left(\frac{\pi}{2} - \psi + \phi\right) - C * AB * \cos(\psi) + C * CD * \cos(\theta) - k_h W_1 - k_h W_2$$
$$- R\cos\left(\frac{\pi}{2} - \theta + \phi\right) = 0 \qquad (15)$$

$$(P_{a3LH})\sin(\delta) + P_{a2LH} * \sin\left(\frac{\pi}{2} - \psi + \phi\right) + C * AB * \sin(\psi) + C * CD * \sin(\theta) - (1 - k_v)W_1$$
$$- (1 - k_v)W_2 - R\sin\left(\frac{\pi}{2} - \theta + \phi\right) = 0 \qquad (16)$$

Multiplying the first equation (15) by $\sin\left(\frac{\pi}{2} - \theta + \phi\right)$ and the second equation (16) by $\cos\left(\frac{\pi}{2} - \theta + \phi\right)$ and summing them gives :

$$P_{a2LH} = \frac{1}{2} * \gamma H^2 * \{-\frac{\sin\left(\frac{\pi}{2} - \theta + \phi + \delta\right)}{\sin(\pi - \theta + 2\phi - \psi)} * \left(K_{a\gamma 3LH}\right)$$
$$+ \frac{(1 - \alpha)^2 * \cot(\psi) + \cot(\theta)}{\sin(\pi - \theta + 2\phi - \psi)}\left[k_h \sin\left(\frac{\pi}{2} - \theta + \phi\right) + (1 - k_v)\cos\left(\frac{\pi}{2} - \theta + \phi\right)\right]\} - CH$$
$$* \frac{1}{\sin(\pi - \theta + 2\phi - \psi)}\{[(\cot(\theta) * \sin\left(\frac{\pi}{2} - \theta + \phi\right)$$
$$+ \cos\left(\frac{\pi}{2} - \theta + \phi\right) * (2 - \alpha) - (1 - \alpha) * \cot(\psi) * \sin\left(\frac{\pi}{2} - \theta + \phi\right)]\}$$
$$= \frac{1}{2}\gamma H^2 * K_{a\gamma 2LH} - CHK_{ac2LH} \qquad (17)$$

At this level, we have determined the analytical formulas for the various active dynamic thrust coefficients according to the geometry of the Cantilever wall (short heel and long heel). However, the question is: how can we know whether the failure mechanism behind the wall corresponds to that of a wall with a short heel or that of a wall with a long heel?
Greco [4] suggests maximizing the lateral dynamic thrust force or minimizing the vertical dynamic force to answer this question.
Thus, the problem is to determine the values of ψ and θ maximizing the following function: Pae(ψ,θ)= Pa1(ψ,θ)+Pa2(ψ,θ)+Pa3(ψ,θ).
As this is a force whose formula varies according to the failure mechanism, it is necessary to consider the critical case illustrated in Figure 9.

The value of the angle ψ_crt=arctan((1-α)/β).

Initially, it is assumed that the failure mechanism corresponds to that of a wall with a short heel. After determining the value of ψ and θ, we compare ψ with the value of ψ_crt and two cases arise: ψ< ψ_crt: the failure mechanism effectively corresponds to that of a wall with short heel and we thus obtain the values of ψ, θ and Pae; ψ> ψ_crt: the failure mechanism corresponds to that of a wall with a long heel, and the formulas adapted to this case are used to derive the values of ψ, θ and Pae.

The maximization procedure used at this stage is performed with Microsoft Excel.

To obtain mathematically consistent results, upper and lower limits are used for certain parameters in derived formulas. Upper and lower bounds are defined by the following conditions: θ > Φ, ψ + θ > 2Φ.

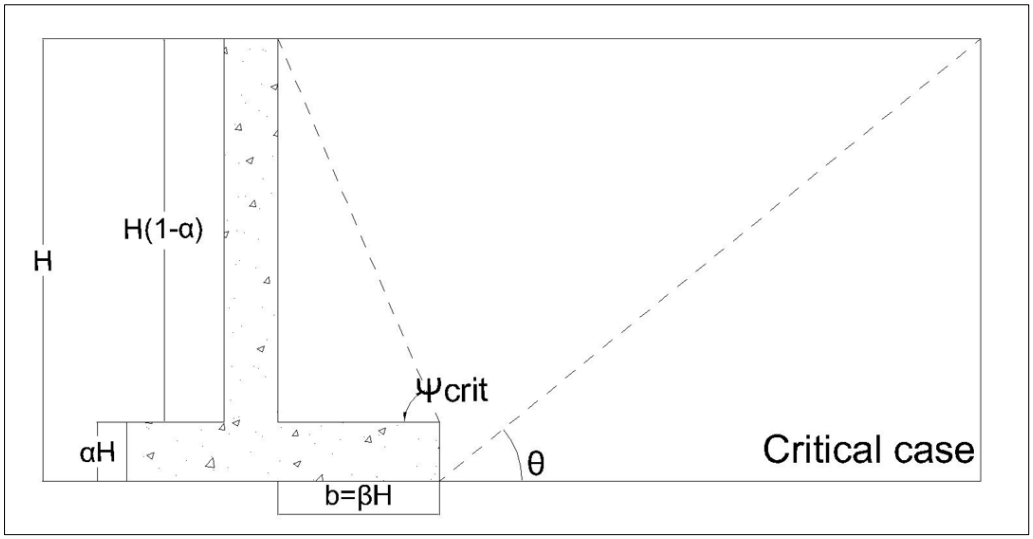

Figure 9. the critical case separating the two cases (wall with short heel and wall with long heel)

III. RESULTS

The results presented in this paragraph are obtained by applying the above formulas to two examples: one example of a cantilever wall with a short heel and another example of a cantilever wall with a long heel. The geometric characteristics of the two walls are shown in Table 1.

Table 1. Geometric characteristics of the two cantilever retaining walls (Short Heel and Long Heel)

	Cantilever wall with Short Heel	**Cantilever wall with long Heel**
α	0,05	0,07
β	0,14	0,35
H	7m	7m
Thickness	0,40m	0,40m

In both cases, the cantilever wall supports a backfill soil with the following mechanical characteristics: Φ=30°, γ=18 KN/m3. The parametric study was mainly based on two parameters: the horizontal seismic

coefficient Kh and the cohesion C (the vertical seismic coefficient is not taken into account). Three cohesion values are considered: C = 0 kPa, C = 10 kPa, and C = 20 kPa.
The results obtained will be compared with those from the following methods: Okabe and Mononobe [11-12], Puri et al., 2004 [13], Shukla 2014 [17] and Iskander et al. [7] and illustrated in Figures 10, 11, and 12. The results for a long-heel wall are shown in Figures 13, 14, and 15.

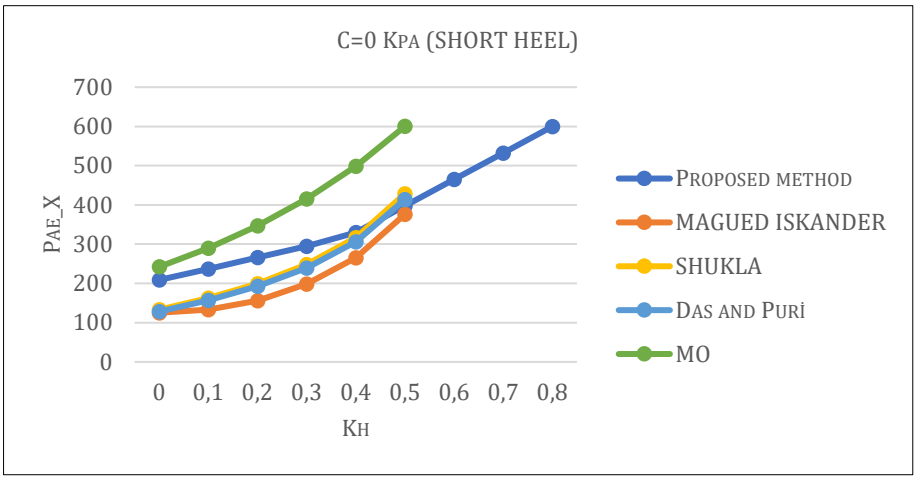

Figure 10. The variation of the horizontal component of the active dynamic force obtained by the proposed formula and the other formulas (C=0Kpa, Short Heel)

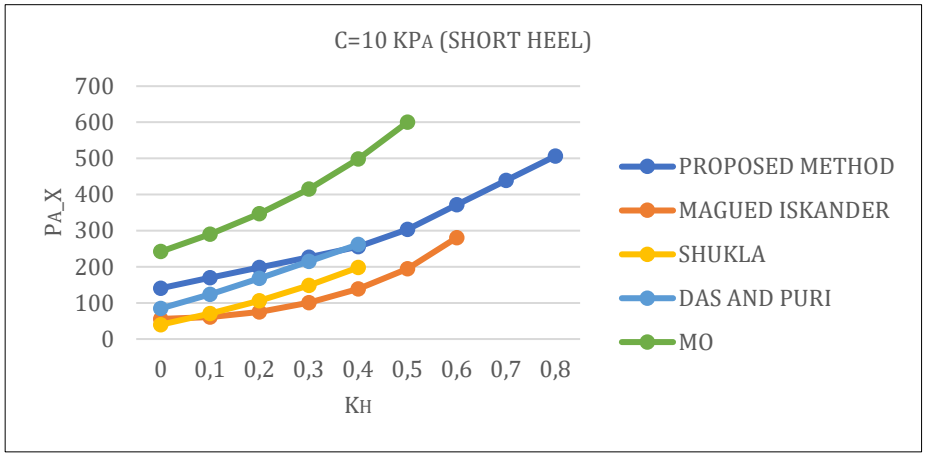

Figure 11. The variation of the horizontal component of the active dynamic force obtained by the proposed formula and the other formulas (C=10Kpa, Short Heel)

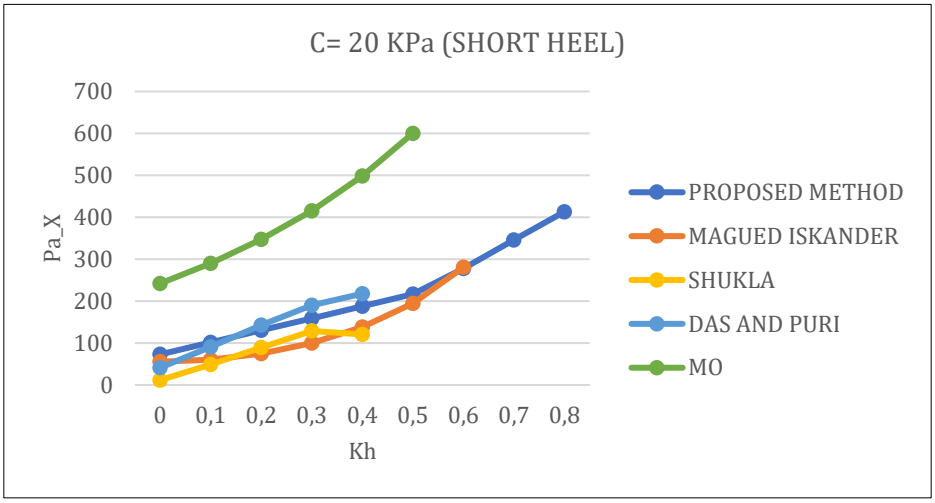

Figure 12. The variation of the horizontal component of the active dynamic force obtained by the proposed formula and the other formulas (C=20Kpa, Short Heel)

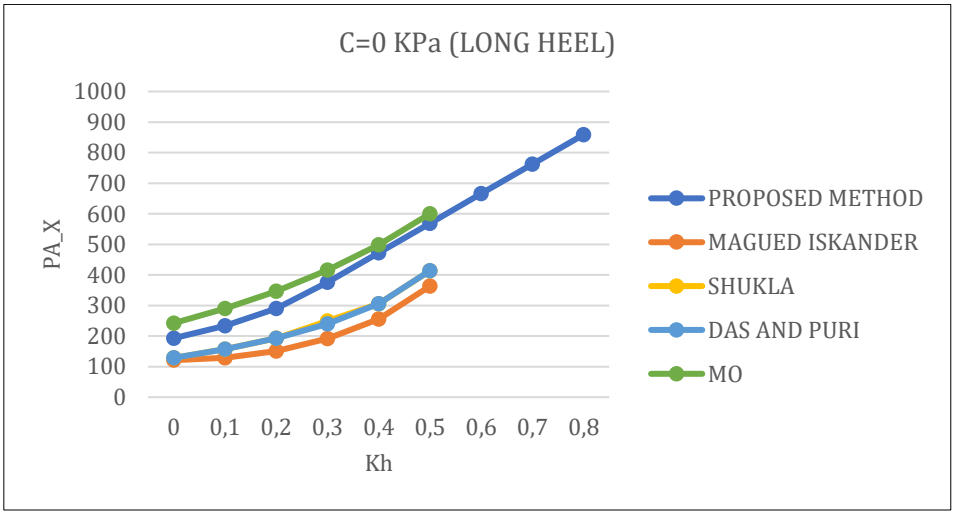

Figure 14. The variation of the horizontal component of the active dynamic force obtained by the proposed formula and the other formulas (C=0Kpa, Long Heel)

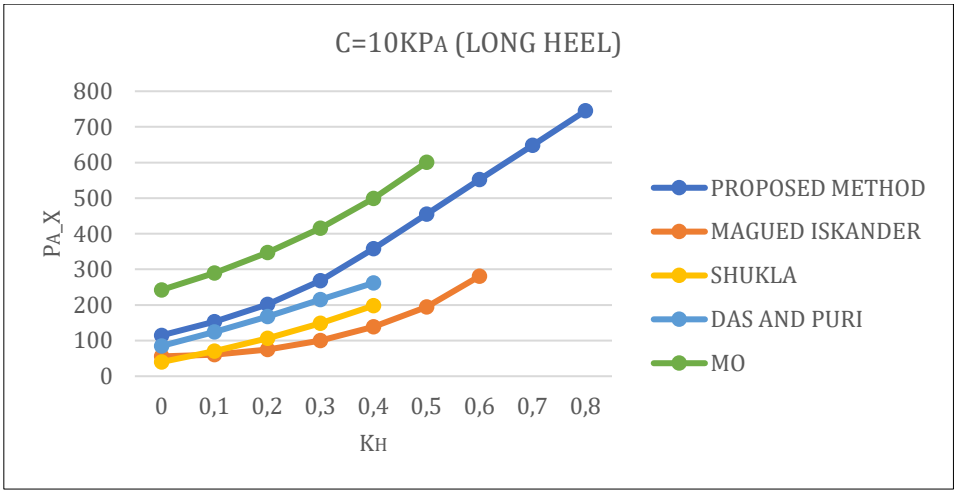

Figure 15. The variation of the horizontal component of the active dynamic force obtained by the proposed formula and the other formulas (C=10Kpa, Long Heel)

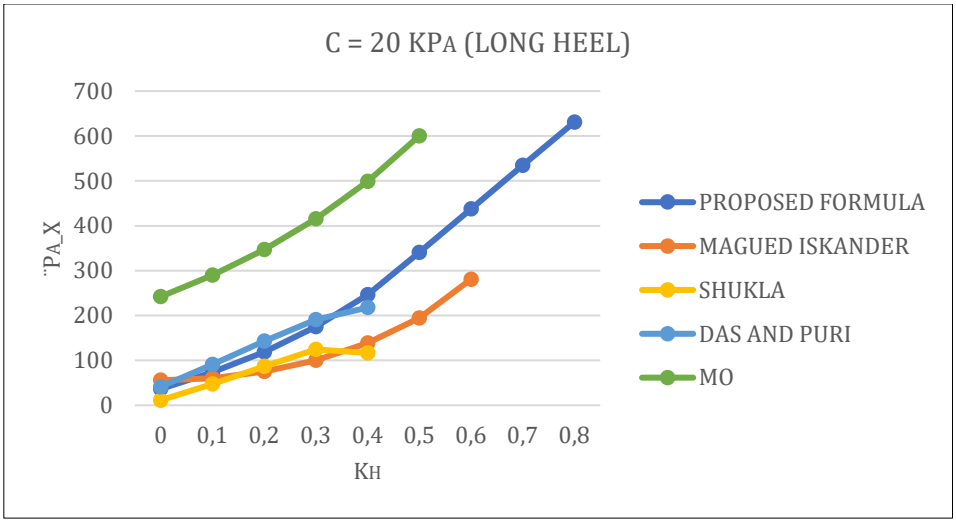

Figure 15. The variation of the horizontal component of the active dynamic force obtained by the proposed formula and the other formulas (C=20Kpa, Long Heel)

IV. DISCUSSION

Analysis of the graphs showing the results obtained in the case of a wall with a short heel is as follows:

- The proposed formula provides more conservative results than the pseudo-static methods [11,12,13,17] for low- to moderate-intensity earthquakes, for which the Kh coefficient varies between 0.1 and 0.4, with a 25% increase in active dynamic force;
- For strong earthquakes (kh>0.5g), the proposed formula became competitive as other methods are not defined for this range of Kh values;
- Compared with the Iskander [7] method based on the Rankine approach [14] (stress field analysis), the proposed formula provides more conservative results (70% increase for weak earthquakes (Kh between 0.1 and 0.3). For Kh between 0.3 and 0.4, the difference becomes minimal;
- The proposed formula provides less conservative values of 35% than the MO formula [11-12];
- For low-intensity earthquakes (Kh between 0.1 and 0.3), slip surfaces with a short heel are inclined at angles of $\theta=60°$ and $\psi=55°$;
- In the case of medium-to-strong earthquakes (Kh >0.4), slip surfaces in the case of a short heel are inclined at angles of $\theta=35°$ and $\psi=55°$;
- In the case of low-cohesion soils and for medium-intensity earthquakes (Kh between 0.35 and 0.5), the results obtained by the proposed formula and those of other methods converge;
- As cohesion increases, the active dynamic force decreases;
- Cohesion does not affect sliding surface inclination angles.

Analysis of the graphs showing the results obtained in the case of a wall with a long heel is as follows:

- The proposed formula provides more conservative results than the pseudo-static methods [13,17] for low- to moderate-intensity earthquakes, for which the Kh coefficient varies between 0.1 and 0.4, with a 45% increase in active dynamic force;
- For strong earthquakes (kh>0.5g), the proposed formula became competitive as other methods are not defined for this range of Kh values;
- Compared with the Iskander [7] method based on the Rankine approach[14] (stress field analysis), the proposed formula provides more conservative results (70% to 80% increase);
- The proposed formula provides values that are 50% less conservative than the MO formula [11-12];
- As cohesion increases, the active dynamic force decreases;

- Cohesion does not affect sliding surface inclination angles.

V. CONCLUSION

- For low- to medium-intensity earthquakes (Kh between 0.1g and 0.5g), the proposed formula provides an upper limit of dynamic thrust values to be taken into consideration in the case of 'sensitive' retaining structures where the risk of collapse must be minimized (densely populated areas, areas close to schools, etc.);
- The strength of the proposed formula is that it provides dynamic thrust values for medium to strong earthquakes (Kh>0.5g) where other pseudo-static methods are not defined.Also, the proposed formula provides, in addition to the thrust force, the shape and angles of the sliding surfaces;
- Increasing the cohesion of the retained soil leads to a decrease in the active thrust force;
- In the case of the Cantilever wall, it is necessary to take into account the shape of the sliding surfaces, which varies according to the geometry of the heel;
- For the same wall height, it is advisable to opt for long heels ($\beta > 0.3$), which improve stability against overturning and reduce the dynamic thrust force;

REFERENCES

1. Anderson, D. G., Martin, G. R., Lam, I. P., & Wang, J. N. (2008). Seismic analysis and design of retaining walls, buried structures, slopes, and embankments. National Cooperative Highway Research Program (NCHRP), Transportation Research Board. Report 611.
2. Coulomb, C. A. (1776). Essai sur une application des règles de maximis et minimis quelques problèmes de statique, relatifs à l'architecture. Memoires de Mathematique de l'Academie Royale de Science, 7, 3-38.
3. Cheng YM. (2003). Seismic lateral earth pressure coefficients for c–φ soils by slip line method. Comput Geotech, 30(8), 661–70.
4. Greco, V. R. (2001). Active earth thrust on cantilever walls with short heel. Canadian Geotechnical Journal, 38(2), 401–409.
5. Greco, V. R. (2007). Reexamination of Mononobe-Okabe Theory of Gravity retaining walls using centrifuge model tests. Soils and Foundations, 47(5), 999–1001.
6. Gupta, A., Chandaluri, V. K., Sawant, V. A., & Shukla, S. K. (2016). Development of design charts for the dynamic active thrust from c–φ soil backfills. In Indian Geotechnical Conference (IGC2016), Chennai, India.
7. Iskander, M., Chen, Z., Mehdi Omidvar, Guzman, I. L., & Elsherif, O. (2013). Active static and seismic earth pressure for c–φ soils. Soil Dynamics and Earthquake Engineering, 53(5), 639–652.
8. Kamiloğlu, H. A., & Şadoğlu, E. (2014). Experimental examination of active and passive wedge in backfill soil of model cantilever retaining wall. International Journal of Structural Analysis & Design, 1(3), 96-100.
9. Kamiloğlu, H. A., & Şadoğlu, E. (2019). A method for active seismic earth thrusts of granular backfill acting on cantilever retaining walls. Soils and Foundations, 59(2), 419–432.
10. Mazindrani, Z. H., & Ganjali, M. H. (1997). Lateral earth pressure problem of cohesive backfill with inclined surface. ASCE Journal of Geotechnical and Geoenvironmental Engineering, 123(2), 110–2.
11. Mononobe, N., & Matsuo, H. (1929). On the determination of earth pressures during earthquakes. In Proceedings, World Engineering Congress, Tokyo, Japan, 1929 (Vol. 9, p. 177–185). Paper No. 388.
12. Okabe, S. (1926). General theory of earth pressures. Journal of the Japanese Society of Civil Engineers, 12(1).
13. Puri, V. K., Prakash, S., & Widanarti, R. (2004). Retaining walls under seismic loading. In Proceedings of the fifth international conference on case histories in geotechnical engineering, 2004, New York, NY, April 13-17, 2004 (p. 7).
14. Rankin, W. (1857). On the stability of loose earth. Philosophical Transactions of the Royal Society, London, 147, 9–27.
15. Salem, A. N., Ezzeldine, O., & Amer, M. R. (2020). Seismic loading on cantilever retaining walls: Full-scale dynamic analysis. Soil Dynamics and Earthquake Engineering, 130, 105962.
16. Shrestha, S., Ravichandran, N., Raveendra, M., & Attenhofer, J. A. (2016). Design and analysis of retaining wall backfilled with shredded tire and subjected to earthquake shaking. Soil Dynamics and Earthquake Engineering, 90, 227–239.
17. Shukla, S. K. (2014). Generalized analytical expression for dynamic active thrust from c–φ soil backfills. International Journal of Geotechnical Engineering, 9(4), 416–421.
18. Shukla, S. K., Gupta, S. K., & Sivakugan, N. (2009). Active earth pressure on retaining wall for c-φ soil backfill under seismic loading condition. ASCE Journal of Geotechnical and Geoenvironmental Engineering, 135(5).
19. Shi, H., Jinxing, G., & Yqing, Z. (2016). Earth pressure of layered soil on retaining structures. Soil Dynamics and Earthquake Engineering, 83, 33–52.